

In vivo up-regulation of aryl hydrocarbon receptor expression by 2,3,7,8-tetrachlorodibenzo-*p*-dioxin (TCDD) in a dioxin-resistant rat model[☆]

Monique-Andrée Franc^a, Raimo Pohjanvirta^{b,c,d}, Jouko Tuomisto^b, Allan B. Okey^{a,*}

^aDepartment of Pharmacology, University of Toronto, Medical Sciences Building, 1 King's College Circle, Toronto, Ontario M5S 1A8, Canada

^bNational Public Health Institute, Department of Environmental Medicine, Kuopio, Finland

^cNational Veterinary and Food Research Institute, Regional Laboratory of Kuopio, Kuopio, Finland

^dDepartment of Food and Environmental Hygiene, Faculty of Veterinary Medicine, University of Helsinki, Helsinki, Finland

Received 19 January 2001; accepted 14 May 2001

Abstract

The aryl hydrocarbon receptor (AHR) mediates toxicity of 2,3,7,8-tetrachlorodibenzo-*p*-dioxin (TCDD) and regulates expression of several genes such as *CYP1A1*. Little is known about what regulates expression of the AHR itself. We tested the ability of TCDD to alter *in vivo* expression of its own receptor in rat strains that are susceptible to TCDD lethality [Long-Evans (*Turku AB*) (L-E) and Sprague Dawley (SD)] and in a rat strain that is remarkably resistant to TCDD lethality [Han/Wistar (*Kuopio*) (H/W)]. Rats were administered a single, intragastric dose of 5 or 50 $\mu\text{g/kg}$ of TCDD. Hepatic cytosol, nuclear extract, and RNA were prepared at 1, 4, and 10 days after TCDD exposure. AHR expression was assessed at three levels: ligand binding function, immunoreactive protein and mRNA. TCDD at 5 $\mu\text{g/kg}$ produced a 2- to 3-fold increase in cytosolic AHR in all strains; 50 $\mu\text{g/kg}$ produced depletion at day 1 followed by recovery in SD and H/W but not L-E rats. Both the increase in AHR above basal levels and the recovery from initial depletion were accompanied by elevations in steady-state AHR mRNA, suggesting a pre-translational mechanism for AHR regulation by its own ligand. This up-regulation *in vivo* is in contrast to the sustained depletion of AHR caused by TCDD in cell culture. There was no clear relationship between AHR regulation and strain sensitivity; thus, the large inherent strain differences in susceptibility to TCDD lethality probably are not explained by differential regulation of AHR by TCDD. © 2001 Elsevier Science Inc. All rights reserved.

Keywords: Aryl hydrocarbon receptor; 2, 3, 7, 8-Tetrachlorodibenzo-*p*-dioxin; Up-regulation; Rat; Dioxin-resistance model; TCDD

1. Introduction

The AHR is an intracellular protein that binds specific aromatic hydrocarbons including environmentally important halogenated aromatic hydrocarbons, non-halogenated polycy-

clic aromatic hydrocarbons, and aromatic amines [1]. Ligand binding liberates the AHR from its chaperone proteins, enabling it to translocate into the nucleus where it exists heterodimerized with its partner protein ARNT. The ligand · AHR · ARNT complex enhances transcription of a battery of genes including *CYP1A1*, *1A2*, and *1B1*, and glutathione-*S*-transferase Ya subunit [2,3]. The mechanism of altered gene expression via DREs has been investigated in great detail for genes such as *CYP1A1* [1,2], but little is known about what regulates expression of the AHR itself, particularly *in vivo*.

TCDD is a potent, high-affinity ligand for the AHR. At exceptionally low doses, TCDD produces an extensive list of adverse effects including immune suppression, liver toxicity, endocrine disruption, teratogenesis, carcinogenesis, and severe anorexia-like wasting [4]. The pivotal role of the AHR in mediating TCDD toxicity is supported by several lines of evidence ranging from classical receptor theory

[☆] Portions of this work were presented at the 20th International Symposium on Halogenated Environmental Organic Pollutants & POPS, Monterey, California (August 13–17, 2000).

* Corresponding author. Tel.: +1-416-978-7243; fax: +1-416-978-6395.

E-mail address: allan.okey@utoronto.ca (A.B. Okey).

Abbreviations: AHR, aryl hydrocarbon receptor; AP, alkaline phosphatase; ARNT, aryl hydrocarbon receptor nuclear translocator protein; dNTP, 2'-deoxynucleoside 5'-triphosphate; DRE, dioxin responsive element; H/W, Han/Wistar (*Kuopio*); L-E, Long-Evans (*Turku AB*); PCB, polychlorinated biphenyl; PCR, polymerase chain reaction; RT, reverse transcription; SD, Sprague Dawley; and TCDD, 2,3,7,8-tetrachlorodibenzo-*p*-dioxin.

[5,6] and Mendelian genetics [7] to contemporary gene knockouts [8,9]. Notwithstanding extensive toxicological data, the cause of TCDD-induced death in animals remains unclear as do the target tissue(s) and organ(s) that are integral to acute lethality.

There exists a broad range of susceptibility to the biochemical and toxic effects of TCDD across species, individuals, and tissues [10]. Within the same species, the “non-responsive” DBA/2 mouse can endure a 10-fold greater dose of TCDD than its C57BL/6 “responsive” counterpart [6]. This is true for lethal effects as well as biochemical/histological changes and is explained primarily by a lower ligand binding affinity [11] due to a mutation in the ligand binding domain of the DBA/2 receptor [12].

A dramatically greater strain difference in TCDD lethality exists in rats. The Han/Wistar (*Kuopio*) rat can withstand a 1000-fold greater dose of TCDD than the Long-Evans (*Turku AB*) rat [13]. In contrast to the mouse model, AHRs in L-E and H/W rats have similar binding affinities for TCDD, and many of their biochemical and toxicological responses (including CYP1A1 induction) appear nearly identical [4,14]. However, L-E and H/W rats express AHR proteins of different sizes [14]. Recent molecular cloning of the receptor from these strains revealed a deletion/insertion-type mutation at the intron 10/exon 10 junction generating splice variants in the resistant H/W rat. This results in deletion of a segment of 38 or 43 amino acids within the *trans*-activation domain of the receptor [15]. The impact of this deletion on signaling in pathways leading to TCDD lethality remains unknown, but genetic studies have established a major role for this variant in resistance to acute TCDD lethality [7].

Alterations in cellular abundance of AHR potentially could modify the ultimate response to TCDD. Consequently, differences in regulation of expression of the AHR may contribute to differential TCDD susceptibility. Several agents affect the level of AHR in cells and tissues [10]. Phenobarbital in mice and rats [16], Aroclor 1254 (a PCB mixture) [17] and *trans*-aminostilbene [18] in rats were all shown to elevate AHR levels. Landers *et al.* [19,20] and Benedetti *et al.* [21] reported that the AHR-like protein induced by 2,2',4,4',5,5'-hexachlorobiphenyl, phenobarbital, or TCDD was kinetically distinct from (but structurally similar to) the AHR. Sloop and Lucier [22] and Bunce *et al.* [23] reported elevations in rodent cytosolic AHR following TCDD treatment *in vivo*, as quantitated by radioligand binding. Conversely, by immunoblotting Pollenz *et al.* [24] observed depletion of whole-cell AHR in multiple tissues after *in vivo* treatment with TCDD. In mouse hepatoma cells grown in culture, TCDD treatment leads to down-regulation of the AHR [25–28]. In cultured cells, AHR levels also decline following exposure to staurosporine [29]. Agents such as transforming growth factor- β_1 have been shown to regulate AHR expression levels in a cell-specific manner [30].

The goals of our current study were 2-fold: (i) to determine the effects of TCDD on AHR levels *in vivo* using

multiple and independent approaches to measure AHR expression following TCDD exposure; and (ii) to investigate a potential mechanism for differential TCDD susceptibility in the rat model, namely, a possible differential pattern or degree of regulation of expression of the AHR by TCDD in the TCDD-sensitive L-E and Sprague Dawley (SD) versus resistant H/W rats.

2. Materials and methods

2.1. Reagents and solutions

The TCDD used to treat animals was purchased from the UFA-Oil Institute and was > 99% pure as determined by gas chromatography–mass spectrometry [31]. TCDD was dissolved in ether and added to corn oil; the ether was subsequently evaporated off. [^3H]TCDD for binding assays (40 Ci/mmol, chemical purity > 97%) was purchased from Chemsyn Science Laboratories. 2,3,7,8-Tetrachlorodibenzofuran was a gift from Dr. Stephen Safe (Texas A&M University). HEGD = 25 mM HEPES, 1.5 mM EDTA, 10% (v/v) glycerol, 1 mM dithiothreitol (pH 7.4); TNT = 20 mM Tris base, 137 mM NaCl, 0.5% Tween (pH 8.0); 1 \times Qiagen Taq DNA polymerase reaction buffer contained Tris \cdot Cl, KCl, $(\text{NH}_4)_2\text{SO}_4$, 1.5 mM MgCl_2 ; 5% (w/v) “blocking reagent” (Vistra ECF Western Blotting Kit, Amersham) for immunoblotting was prepared in TNT.

2.2. Antibodies

Anti-AHR polyclonal antibody (from rabbit) was obtained from Biomol Research Laboratories, Inc. (Catalog No. SA-210); this antibody was raised against amino acids 1–402 of the mouse *Ah^{b-1}* allele [32]. Anti-ARNT antibody for pilot ARNT immunoblotting was provided by Dr. O. Hankinson. This antibody was raised against amino acids 399–777 of the human ARNT sequence.

2.3. Animals

Female SD rats, inbred L-E rats, and outbred H/W rats (all 10- to 12-weeks-old) were obtained from the breeding colony of the National Public Health Institute, Division of Environmental Health. Animals were kept in stainless steel wire-mesh cages, 5 rats per cage, and allowed unlimited access to standard pelleted animal feed (R36, Ewos) and tap water. Lights were on between 7:00 a.m. and 7:00 p.m. Ambient room temperature and humidity were maintained at $21.5 \pm 1^\circ$ and $55 \pm 10\%$, respectively.

2.4. Animal treatment and tissue harvest

Rats were given a single dose of 5 or 50 $\mu\text{g/kg}$ of TCDD or corn oil vehicle alone by gavage. Animals were weighed, and then euthanized by decapitation at 1, 4, or 10 days

post-TCDD administration ($N = 5/\text{treatment group}$). Approximately 1 g of tissue from two lobes of liver was removed, weighed, and immediately submerged in liquid nitrogen for RNA isolation. The remaining liver was weighed and homogenized with a Potter–Elvehjem glass–Teflon homogenizer in 4 vol. of ice-cold HEGD buffer (20% homogenate) for preparation of subcellular fractions.

2.5. Subcellular fractions

Subcellular fractions were prepared by differential centrifugation as described by Mason and Okey [33] with the following modifications: nuclear proteins were extracted with 0.5 M NaCl-HEGD (pH 8.5); subcellular fractions were stored in liquid nitrogen; total protein was measured in triplicate by the Bradford protein assay [34] using bovine serum albumin as the protein standard. Whole tissue lysates were prepared as described by Pollenz *et al.* [24]. Lysates were prepared from a single animal from both control and treated (day 10; 5 and 50 $\mu\text{g/kg}$) groups of each strain.

2.6. Radioligand binding

Radioligand binding and protein separation on sucrose density gradients were performed as previously described [14]. The 10 nM [^3H]TCDD incubating radioligand concentration was selected based on saturation analyses performed on control and treated (day 10; 5 $\mu\text{g/kg}$) SD rats.

2.7. Immunoblotting

Proteins from cytosol or nuclear extract were separated by Tris-glycine sodium dodecyl sulfate polyacrylamide (6%) gel electrophoresis (SDS–PAGE). Protein loading per lane was identical for each sample within a strain and was: 75 μg for SD and L-E cytosol, 150 μg for H/W cytosol, and 100 μg for all nuclear extracts. Gels were electroblotted onto a polyvinylidene difluoride membrane (Immobilon-P, Millipore Corp.) (100 V; 1 hr). Protein transfer was assessed by Ponceau S staining. “Blocked” membranes were incubated sequentially with primary and secondary antibodies and with the AP conjugate with gentle agitation at ambient temperature. Antibodies were diluted in blocking reagent as follows: *Cytosols*: AHR antibody = 0.003 $\mu\text{g/mL}$; fluorescein-linked anti-rabbit antibody = 1:10,000. *Nuclear extracts*: AHR antibody = 0.02 $\mu\text{g/mL}$; fluorescein-linked anti-rabbit antibody = 1:2500. The antiluorescein–alkaline phosphatase conjugate was diluted in TNT = 1:2500. Three changes of TNT buffer for a total of 30 min were used to wash membranes between incubations. The AP-catalyzed fluorescence was initiated by the addition of approximately 50 $\mu\text{L/cm}^2$ of AttoPhos fluorescent substrate (Amersham) (10 min). Fluorescent emissions were captured using a Storm Phosphorimager (Molecular Dynamics). Signal strength (with subtraction of background at the band perimeter) was calculated with IPLab Gel H band quantitation

software. To ensure the quantitative nature of the immunoblotting assay, experimental parameters were optimized such that extremes in AHR levels were within the linear range of the assay. Antibody concentrations and incubation times, the total amount of sample protein loaded, and fluorescence detection parameters were optimized accordingly. All samples of each strain ($N = 40/\text{strain}$) were immunoblotted simultaneously. To minimize positional effects on the gel, samples were assigned randomly to lanes. To allow comparison between gels, signal strength was normalized to the mean of signal intensities of duplicate normalization standards (prepared by pooling day 1 control cytosols or nuclear extracts of the corresponding rat strain) loaded onto each gel. AHR immunoreactive protein was not normalized to an internal standard (such as β -actin) since total protein has been shown previously to be an adequate denominator for similar AHR measurements [24,27,35,36]. Assays were performed in duplicate with satisfactory agreement between duplicate data, and results are expressed as the mean of the duplicates. The AHR receptor band was positively identified by (i) comparison of known molecular weight with cytosols from Hepa-1 mouse cells and LS180 human cells [25,37], (ii) molecular weight difference (106 vs 98 kDa) in SD and L-E vs H/W AHRs [14], and (iii) covalent linkage of the cytosolic AHR (photoaffinity labelling) with [^3H]TCDD [38].

For measurement of ARNT protein levels in cytosol, antibodies were diluted in blocking reagent as follows: ARNT-specific polyclonal antibody = 0.05 $\mu\text{g/mL}$; fluorescein-linked anti-rabbit antibody = 1:5000; and AP = 1:2500 (diluted in TNT).

2.8. RNA isolation

Total RNA was isolated from frozen tissue using TRIzol[®] Reagent (7%, w/v) (on ice; 60 sec) (Gibco BRL/Life Technologies) according to the instructions of the manufacturer. Contaminating DNA was enzymatically degraded with 15 U DNaseI (37°, 20 min + 55°, 10 min) (FPLCpure, Pharmacia Biotech). A crude measure of total RNA yield was calculated from the spectrophotometric absorbance at 260 nm (A_{260}). An $A_{260/280} > 1.7$ was deemed an acceptable measure of RNA purity from tissue. RNA integrity was estimated by visual examination of two distinct ribosomal RNA bands (28S and 18S) on an ethidium bromide-1% agarose gel. Total RNA was re-isolated from samples not meeting quality criteria. RNA was stored at -80° , and integrity was re-confirmed immediately prior to RT–PCR.

2.9. Semi-quantitative RT–PCR

2.9.1. RT

One microgram mRNA was reverse-transcribed to cDNA in a two-step approach using Maloney Murine Leukemia Virus Reverse Transcriptase primed by an oligo(dT) primer as previously described [37]. cDNA was stored for

Table 1

Primer sequences and thermal cycling conditions for the four genes amplified by PCR

Target	Amplimer sequences	Thermal cycling parameters (sec/°) (denature) (anneal) (extend) × cycles
AHR	5'- 714-AGGGAGGTTAAAGTATCTTCATGGAC-739 -3' 5'- 1630-TCCCTAGGTTTCTCATGATGCTATAC-1605 -3'	(20sec; 94°)(20sec; 54°)(40sec; 72°) × 24
1A1	5'- 627-ACGTTATGACCACGATGACC-646 -3' 5'- 1299-AGGCCGGAACCTCGTTT-1283 -3'	(20sec; 94°)(20sec; 52°)(40sec; 72°) × 17
ARNT	5'- 877-CTTGGCTCTGTGAAGGAAGG-896 -3' 5'- 1289-CGGAATCGGAACATGACAG-1271 -3'	(20sec; 94°)(19sec; 53°)(40sec; 72°) × 25
β -ACTIN	5'- 344-ACCGTGAAAAGATGACCCAG-363 -3' 5'- 1031-GAGCCACCAATCCACACAG-1011 -3'	(20sec; 94°)(20sec; 51°)(40sec; 72°) × 16

Accession numbers: AHR = U09000; CYP1A1 = X00469; ARNT = U61184; β -actin = J00691. Sites of primer design are designated according to 1 = A in the first codon (ATG) of the corresponding cDNA.

no longer than 1 week at -80° until used. Sufficient cDNA was synthesized to PCR-amplify all genes (targets and standard) from the same source of cDNA.

2.9.2. PCR

AHR, CYP1A1, and ARNT cDNAs were PCR-amplified, and signals were normalized to the internal reference standard, β -actin. Each cDNA was amplified in a separate tube using Qiagen Taq DNA polymerase. The product of amplification was labeled for detection by incorporation of [α - 32 P]dCTP. The 50- μ L reactions contained cDNA derived from 125 ng RNA; 2.5 U Taq polymerase; 1× PCR reaction buffer; 0.2 μ M of each primer; 0.2 mM of each dNTP; and 1 μ Ci [α - 32 P]dCTP (Amersham Pharmacia Biotech Inc.). Reaction tubes were introduced into a 90° GeneAmp PCR System 9600 (Perkin Elmer). Temperature cycling (Table 1) was flanked by an initial denaturation step (4 min; 94°) and a final extension step (7 min; 72°). PCR product was separated on 10% non-denaturing polyacrylamide gels. Radioactive emissions were captured on a Phosphor screen and digitized by the Storm Phosphorimager SF system. Signal intensity was quantitated using IPLab Gel H software.

Relative rather than absolute levels of gene expression were sought since variation in efficiency of RT and PCR reactions for each sample was undefined and decay of radioisotope was variable between assays. β -Actin was used as an internal reference standard to control for variability in all steps leading up to PCR amplification. The quantitative nature of the polymerase chain reaction to measure relative gene expression was ensured as validated by Murphy *et al.* [39]. The ratio of radiolabelled amplicon of the target to that of the reference standard (from the same cDNA source) was used as the measure of steady-state levels of target mRNA. Experiments were performed in triplicate (from the same total RNA isolate). From RNA isolation to signal detection, all individuals within a rat strain were processed simultaneously. Cycle number and template concentration were selected such that minimum and maximum mRNA levels for each gene were within the exponential range of amplification. In pilot analyses, samples identified as having the

highest and the lowest abundance extremes for each gene and each rat strain were identified and amplified by PCR over a variable number of cycles and over a range of template concentrations (data not shown). For CYP1A1 in untreated animals, no signal was detectable by RT-PCR with 34 cycles of amplification. All comparisons of AHR levels among treatment groups were made separately within each strain.

2.10. Primer design

Amplimers were designed with the Primer software program (Whitehead Institute of Biomedical Research) (version 0.5) and, when possible, pairs were designed to contain intron–exon boundaries to distinguish potential genomic DNA contamination (Table 1). Absence of genomic DNA contamination was ensured by PCR amplification of RNA without RT for the ARNT gene for which a complete rat sequence was unavailable. The Blast program (National Center for Biotechnology Information) was used to ensure specificity of the primers. Primers were commercially synthesized by the ACGT Corp., and concentrations were confirmed spectrophotometrically. Migration of a single band to the expected molecular weight distance on a 10% polyacrylamide gel served to confirm the identity of the PCR products. For each reverse transcription, diethylpyrocarbonate-treated water was used as a negative control for contamination. The expected product sizes were: AHR = 917 bp; CYP1A1 = 672 bp; ARNT = 413 bp; and β -actin = 688 bp.

2.11. Statistical analyses

The results are given as group means \pm standard deviation. A strain-wise comparison of treated animals with the corresponding time-matched control values was performed for the means of treated groups across all variables analyzed at days 1 and 10. Day 4 was a special case because there was no contemporary control group at that time point. Since there occasionally proved to be a statistically significant difference in the control means between day 1 and day 10

samples (as assessed by Student's *t*-test), day 4 values were compared separately with both day 1 and day 10 controls rather than pooling the two controls. Variables with homogeneous variances (directly or after logarithmic transformation; assessed by the Levene test) were analyzed by one-way ANOVA followed by Duncan's multiple range post-hoc test. In the case of non-homogeneous variances, the Kruskal-Wallis non-parametric one-way ANOVA was used followed by the Mann-Whitney U test. The limit for statistical significance was set at 0.05.

3. Results

3.1. AHR levels measured by radioligand binding

The AHR population was quantitated by measuring the apparent number of specific [³H]TCDD binding sites in liver cytosol from TCDD-treated and untreated rats under saturating radioligand conditions; this technique detects unoccupied ligand binding sites only. The portion of cytosolic AHR occupied by the TCDD treatment given *in vivo* is therefore undetectable by this assay. Only the cytosolic fraction was subjected to radioligand binding assays since nuclear receptor is presumed to be ligand-bound from the administered TCDD and therefore unavailable to bind radioligand under standard assay conditions.

Representative radioligand gradient profiles for hepatic cytosols from the day 10 control and TCDD-treated animals are shown in Fig. 1A. The shaded area represents specific binding sites. The visually prominent differences in peak areas between treatment groups illustrate the effect of TCDD on AHR levels. Mean values for the total area under the curve within the specific binding peak for each treatment group are graphically displayed in Fig. 1B. Treatment with 5 µg/kg of TCDD produced a statistically significant elevation in ligand binding by day 10 in all strains; the greatest increase was observed in L-E rats (2×). AHR levels were elevated by 1.6× in H/W and 1.3× in SD rats compared to time-matched controls. Only H/W rats displayed a statistically significant decrease in AHR binding at day 1. The gradual increase in AHR over the course of several days in L-E and H/W rats is clear from the transformed data expressed as a percentage of time-matched controls in Fig. 1C.

The 50 µg/kg dose of TCDD produced a different pattern of ligand binding compared with the 5 µg/kg dose. All strains displayed an appreciable decrease in binding at day 1. In SD and H/W rats, this was followed by a gradual increase over time, resulting in nearly complete recovery (SD rats) and complete recovery (H/W rats) to time-matched control levels by day 10. No recovery was observed in L-E rats in which receptor levels remained depressed to 25% that of controls over 10 days. Recovery in SD and H/W rats, and lack thereof in L-E rats, is apparent

from the transformed data expressed as a percentage of the time-matched controls in Fig. 1C.

We did not perform extensive kinetic binding studies on the AHR from TCDD-treated animals versus control animals. However, the apparent K_d for binding of [³H]TCDD to the AHR by Scatchard plot analyses in cytosol of TCDD-treated (day 10; 5 µg/kg) SD rats did not differ from that of control rats (data not shown).

3.2. AHR levels measured by immunoblotting

Immunoblotting was used as an independent approach to measure AHR protein levels in cytosol and nuclear extract. This method detects AHR protein independent of functional integrity of the receptor. The specific AHR band is indicated by arrows to the left of representative immunoblots in Figs. 2A (cytosol) and 3 (nuclear extract). This band was confirmed to represent the AHR as described in "Materials and methods." The effect of treatment on AHR immunoreactive protein levels under optimized immunoblotting conditions is apparent from the range of band intensities on the immunoblots. Mean normalized values are plotted in Fig. 2B. A 5 µg/kg dose of TCDD produced a statistically significant increase in AHR cytosolic protein by day 10 in all strains with no change observable 1 day following TCDD exposure. The magnitudes of increase at day 10 in the treated rats versus the time-matched controls were: H/W = 3.2×; L-E = 3.0×; and SD = 2.1×. At the higher dose, TCDD consistently produced an initial drop in cytosolic AHR protein followed by recovery to control levels in SD and H/W rats but not in L-E rats. A statistically significant difference between day 1 and day 10 controls was observed in H/W rats. The initial depletion and subsequent recovery of AHR over the course of several days in SD and H/W rats are clear from the transformed data expressed as a percentage of the time-matched controls in Fig. 2C. Patterns in cytosolic AHR levels measured by immunoblotting correlated closely to those obtained in radioligand binding assays ($r^2 = 0.739$, $N = 90$).

Immunoblots for nuclear extracts are presented in Fig. 3. Although AHR could be detected in this subcellular fraction, the signal intensity approached the limits of detection (~20 fmol/mg protein) of the assay and therefore could not be quantitated reliably. A notable observation was a stronger signal detectable in low-dose treated animals compared with the high-dose treated animals. Nuclear AHR was virtually undetectable in most groups.

ARNT protein was detectable in cytosols using anti-ARNT antibody, but insufficient antibody was available to permit rigorous quantitation. The only noteworthy trend was a modest depression in ARNT protein in SD and L-E rats receiving high-dose TCDD; no effect was observed in H/W rats or in the low-dose SD or L-E rats (data not shown).

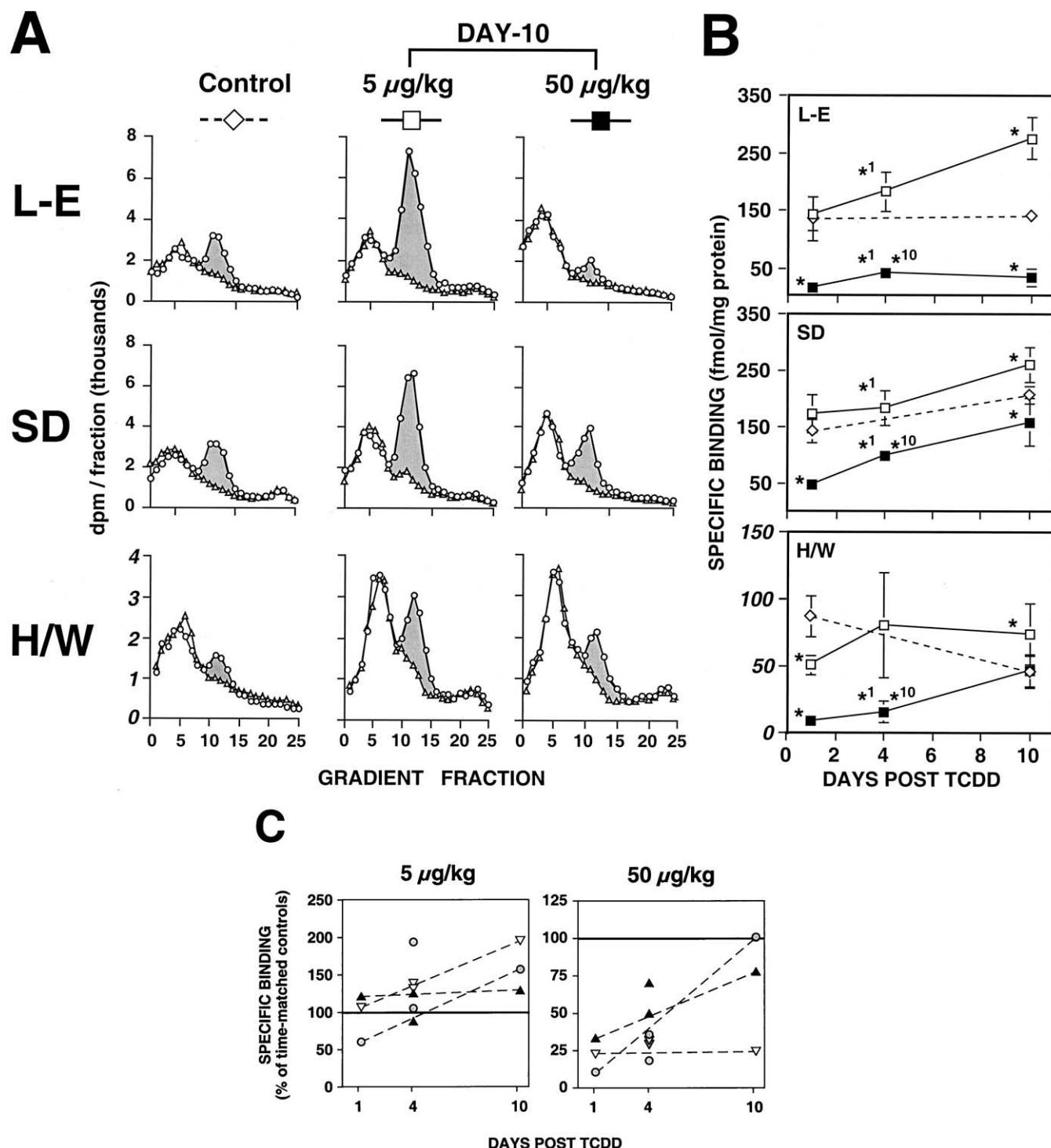


Fig. 1. Radioligand binding in hepatic cytosol of TCDD-treated rats. Cytosols (5 mg/mL protein) were incubated with 10 nM [3 H]TCDD as the radioligand in the absence or presence of a 100-fold molar excess of 2,3,7,8-tetrachlorodibenzofuran as the competitor. Unbound ligand was removed with dextran-coated charcoal and proteins were separated by velocity sedimentation on sucrose density gradients. Gradients were fractionated, and radioactivity was measured in each fraction. (A) Representative radioligand binding profiles from day 10 untreated and treated rats. The shaded area illustrates the specific binding peak. Specific binding was calculated by subtracting binding in the presence of competitor (triangles) from binding in the absence of competitor (circles). (B) Effect of TCDD treatment on radioligand binding (open squares = 5 µg/kg; filled squares = 50 µg/kg; rhombus = corn oil vehicle controls). Specific binding is expressed per mg of total protein (measured in triplicate) in samples analyzed on sucrose gradients. Plotted values are means \pm standard deviation of 5 animals per treatment group. Results for H/W rats are plotted on an expanded scale since constitutive AHR levels are typically half that in L-E rats [14]. Statistically significant difference compared to: (*) = time-matched control; (*1) = day 1 control; and (*10) = day 10 control ($P < 0.05$). (C) Results transformed to percentage of time-matched controls. Day 1 and day 10 transformed data are joined by a dashed line. Day 4 treated animals were divided by both day 1 and day 10 controls and plotted as discrete points for each strain. Open inverted triangles = L-E, filled triangles = SD, and shaded circles = H/W rats.

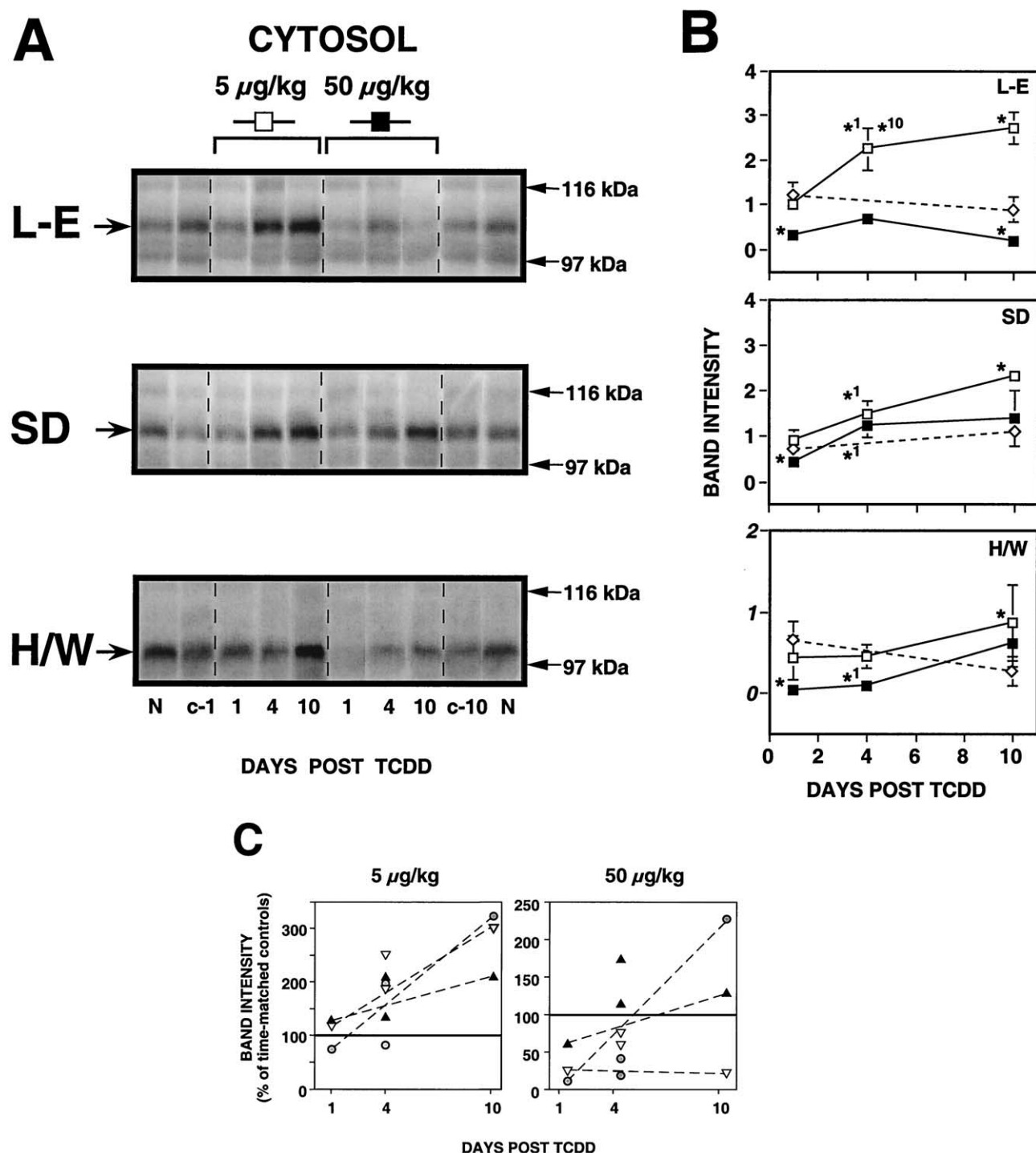


Fig. 2. Immunoblotting for AHR protein in hepatic cytosols of TCDD-treated rats. Cytosolic proteins were separated by SDS-PAGE (L-E and SD = 75 µg total protein per lane; H/W = 150 µg total protein per lane), electrotransferred onto polyvinylidene difluoride membranes, and immunoblotted with an anti-AHR antibody as described in "Materials and methods." (A) Representative immunoblots for AHR: to minimize positional effects, samples were randomly assigned to lanes. For clarity, the illustrated blots were digitally reconstructed by re-organization of lanes from the original blots; signal and background intensities remained intact in the process. Arrows on the left indicate the specific AHR band; positions of molecular weight markers are shown on the right. The AHR migrated to ~106 kDa for L-E and SD and ~98 kDa for H/W. "N" represents the normalization standards (pool of all day 1 controls; 2 per gel) used to normalize sample band intensities. C-1 and C-10 are day 1 and day 10 controls, respectively. (B) Effect of TCDD treatment on AHR protein levels measured by immunoblotting (open squares = 5 µg/kg; filled squares = 50 µg/kg; rhombus = corn oil vehicle controls). Band intensities were normalized to the mean of two normalization standards (N) loaded on the same gel. Plotted values are means ± standard deviation of normalized band intensities (N = 5/treatment group). Assays were performed in duplicate. Results for H/W rats are plotted on an expanded scale since constitutive AHR levels are typically 2-fold less than for L-E rats. Statistically significant difference compared to: (*) = time-matched control; (*1) = day 1 control; (*10) = day 10 control ($P < 0.05$). (C) Results transformed to percentage of time-matched controls. Day 1 and day 10 transformed data are joined by a dashed line. Day 4 treated animals were divided by both day 1 and day 10 controls and plotted as discrete points for each strain. Open inverted triangles = L-E, filled triangles = SD, and shaded circles = H/W strains.

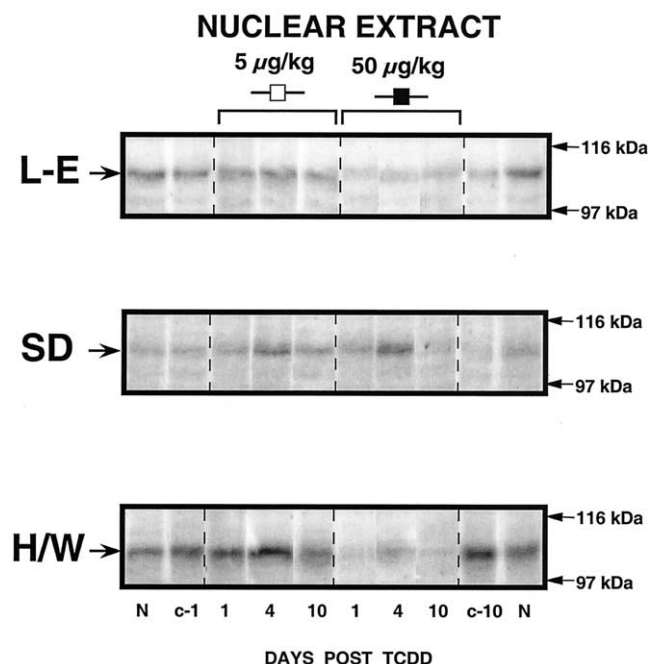


Fig. 3. Immunoblotting for AHR protein in hepatic nuclear extracts of TCDD-treated rats. Nuclear proteins were separated by SDS-PAGE (100 µg total protein per lane), electrotransferred onto PVDF membranes, and immunoblotted with an anti-AHR antibody as described in "Materials and methods" and in the legend to Fig. 2.

3.3. Whole tissue lysates

Other laboratories have measured AHR levels in whole tissue lysates [24,36,40] rather than in cytosol and nuclear extract as in our study. We compared the level of immunoreactive AHR in whole tissue lysates (prepared from several representative samples of control and treated rats) with that of cytosolic fractions from the same tissues. The absolute levels detected were approximately 10-fold less (per same amount of protein) in whole tissue lysates versus their cytosolic counterparts; however, there was a high correlation ($r^2 = 0.945$, $N = 8$) in AHR levels between the two preparations (Fig. 4).

3.4. Effect of TCDD on mRNA levels

3.4.1. Amplification kinetics

The effect of TCDD on AHR expression was assessed at the mRNA level using RT-PCR to measure relative changes in steady-state mRNA. AHR, ARNT, and CYP1A1 were the target mRNAs measured by this approach. Normalization was achieved by independent amplification of the control gene, β -actin, known to be invariant with TCDD treatment. For each gene (target and standard), measurements were derived within the exponential range of amplification (data not shown).

3.4.2. Quantitation

Representative PCR amplicons for each of the sequences are displayed in Fig. 5A. Mean normalized values for the

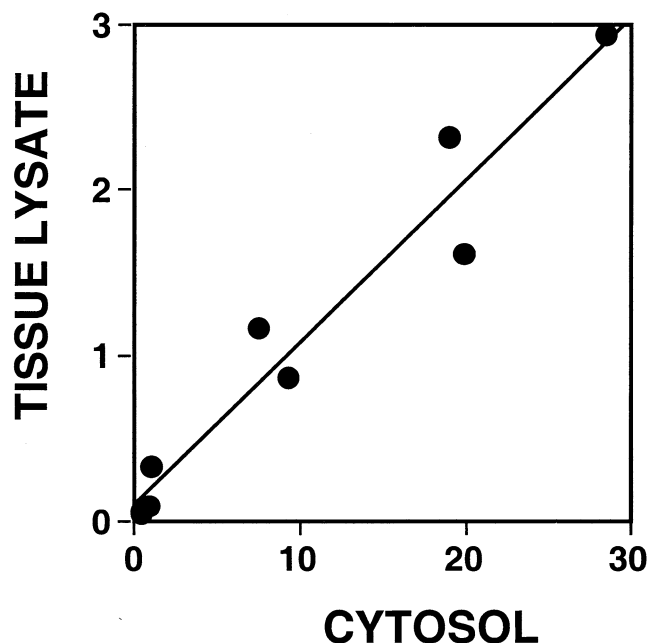


Fig. 4. Comparability of AHR measurements made in whole tissue lysates versus cytosolic fractions. Cytosols and whole tissue lysates prepared from control and treated rats from all strains were immunoblotted for AHR in parallel. For both preparations, 75 µg (SD and L-E) and 150 µg (H/W) of total protein (as determined by triplicate Bradford assays) were separated by SDS-PAGE. Electoblotted membranes were immunoblotted for AHR. Signal intensities from cytosols and whole tissue lysates of the same animal were plotted against each other, and the best-line was fit to the data points, $r^2 = 0.945$, $N = 8$.

target genes are plotted in Fig. 5B. By day 10, AHR mRNA levels were statistically significantly greater than controls following low-dose TCDD in L-E ($2.6\times$) and H/W ($2.3\times$) rats. A significant increase was observed in SD rats at day 4 (when compared to either day 1 or day 10 controls), but levels returned to nearly control levels by day 10. High-dose TCDD produced a significant increase in AHR product levels by day 4, and this substantial elevation was maintained until day 10 (SD = $9.6\times$; H/W = $3.0\times$). Levels of ARNT mRNA were comparatively more stable. At day 1 (5 µg/kg), a small initial drop was observed in L-E and SD rats. L-E rats also showed a decrease in ARNT mRNA at day 10 following the 50 µg/kg dose of TCDD.

CYP1A1 mRNA (used as the biomarker for effectiveness of treatment) was nearly maximally induced by day 1 in all strains. The induction was maintained over the complete time course up to 10 days after TCDD treatment. All strains responded similarly in terms of CYP1A1 induction with the exception of L-E rats that received the high-dose TCDD. In contrast to SD and H/W rats, L-E rats displayed a more modest induction at the high dose than at the low dose. This highly TCDD-sensitive rat strain also showed signs of overt toxicity and an inability to recover from initial depletion of AHR by the high dose. All target mRNA measurements showed a good concordance between day 1 controls and day 10 controls.

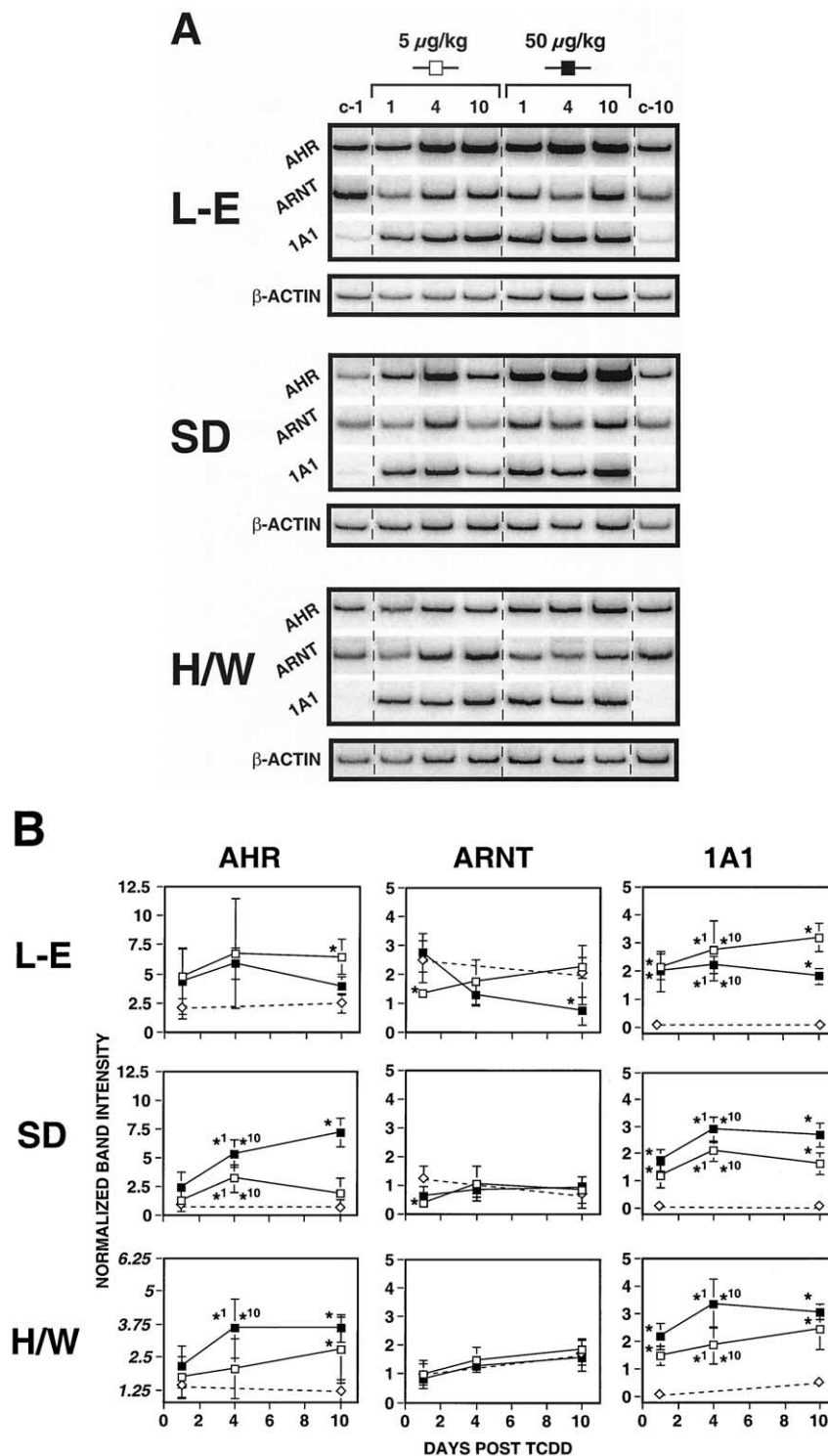


Fig. 5. RT-PCR amplification of AHR, ARNT, and CYP1A1 mRNA from liver of TCDD-treated rats. One microgram of total RNA per sample was reverse-transcribed and PCR-amplified to incorporate radiolabeled [α - ^{32}P]dCTP. PCR product was separated by polyacrylamide gel electrophoresis, and radioactive emissions were captured on a Phosphor screen for detection by a Phosphorimager (see "Materials and methods"). (A) Representative digitized images of radiolabeled PCR product for AHR, ARNT, and CYP1A1 mRNA. PCR product for β -actin, shown separately, was used as an internal normalization standard for the target genes. For clarity of presentation and comparisons, lanes in the image shown were digitally re-organized from original images; band and background intensities were not altered in the process. C-1 and C-10 are day 1 and day 10 controls, respectively. (B) Effect of TCDD treatment on AHR, ARNT, and CYP1A1 mRNA levels (open squares = 5 $\mu\text{g/kg}$; filled squares = 50 $\mu\text{g/kg}$; rhombus = corn oil vehicle controls). Values are group means \pm standard deviation ($N = 5/\text{treatment group}$) of normalized band intensities. Assays were performed in triplicate from the same RNA isolate. Statistically significant difference compared to: (*) = time-matched control; (*1) = day 1 control; and (*10) = day 10 control ($P < 0.05$).

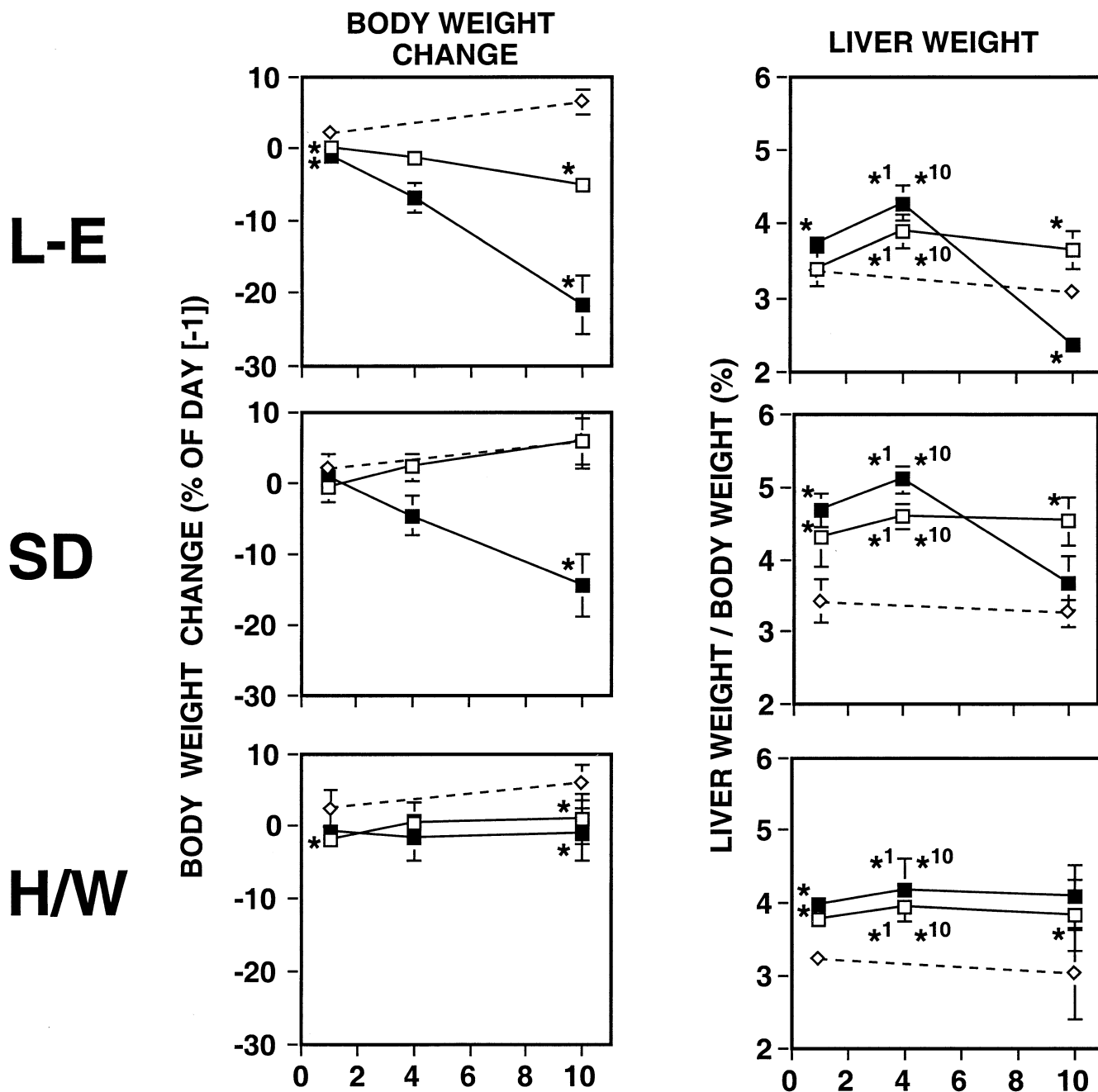


Fig. 6. Body weights and liver weights of female rats treated with TCDD. Body weight measured at time of euthanasia is expressed as a percentage of the initial body weight (measured at day minus-one). Liver weight is expressed as a percentage of the body weight at the time of euthanasia. Open squares = 5 µg/kg, filled squares = 50 µg/kg, rhombus = corn oil vehicle control. Plotted values are means \pm standard deviation of 5 animals per treatment group. Key: (*) = statistically significant difference compared to the time-matched control. For body weights, no comparisons were made for the day 4 time point. For liver weights: statistically significant difference compared to: (*) = time-matched control; (*1) = day 1 control; and (*10) = day 10 control ($P < 0.05$).

3.5. Liver and body weight changes

In addition to the biochemical response of CYP1A1 induction, we measured the effect of TCDD on body weight gain and the liver weight to body weight ratio as a physiological measure of treatment effectiveness. Five micrograms per kilogram of TCDD is below the LD₅₀ for all strains in this study. Fifty micrograms per kilogram of

TCDD exceeds the LD₅₀ for L-E rats by 5-fold and is approximately equal to the LD₅₀ of SD rats. In all strains, control animals showed a 5–6% increase in body weight over the 10-day time course (Fig. 6). The effect of TCDD on body weight differed among strains. Five micrograms per kilogram caused decreased weight gain in L-E rats only; 50 µg/kg caused decreased weight gain in both SD and L-E rats. Neither 5 µg/kg nor 50 µg/kg of TCDD had a signif-

ificant impact on body weight gain of the H/W rats. The corn oil vehicle did not produce any change in the ratio of liver to body weight after 10 days in any strain. However, 5 $\mu\text{g/kg}$ of TCDD produced a measurable increase in the liver/body weight ratio in all strains. The 50 $\mu\text{g/kg}$ dose increased the liver/body weight ratio at day 4, but by day 10 this ratio dropped to or below control values in SD and L-E rats, respectively. This significant decrease in the liver/body weight ratio was observed despite the appreciable decrease in body weight in these strains at the 50 $\mu\text{g/kg}$ dose.

4. Discussion

All three endpoints that we measured—ligand binding, immunoreactive protein, and mRNA levels—lead to the same conclusion: acute exposure of rats to TCDD provokes up-regulation of the AHR receptor in liver over time. We found significant increases above basal expression levels in three rat strains receiving 5 $\mu\text{g/kg}$ of TCDD. With 50 $\mu\text{g/kg}$, AHR protein underwent recovery following an initial depletion at day 1. Increases in AHR protein were invariably accompanied by substantial increases in steady-state AHR mRNA, suggesting that up-regulation of AHR by its own ligand occurs (at least in part) at the pre-translational level.

Previous reports of the effect of TCDD on AHR levels *in vivo* have been contradictory. Sloop and Lucier [22] and Bunce *et al.* [23] reported significant increases in cytosolic AHR levels in rat liver after exposure to TCDD. Each study used radioligand binding to measure receptor content. More recently, several studies using immunoblotting reported depletion of AHR by TCDD in whole tissue lysates of multiple rat tissues [24,36,40]. In the work by Pollenz *et al.* [24], a 10 $\mu\text{g/kg}$ TCDD dose in SD rats produced an initial depletion of AHR immunoreactive protein within hours of oral administration followed by some recovery by 14 days which never re-achieved starting levels in liver. The authors concluded that the AHR is down-regulated by TCDD *in vivo*. In our mapping of AHR expression by TCDD (this study), we found that both 5 and 50 $\mu\text{g/kg}$ of TCDD produced an increase in receptor expression in SD rats, although, at 50 $\mu\text{g/kg}$, this was subsequent to initial depletion in AHR at day 1. The net result was virtually complete recovery of cytosolic receptor levels by day 10. The initial depletion at the high dose (50 $\mu\text{g/kg}$) probably reflects translocation of AHR into the nucleus and subsequent receptor degradation. Despite the likely increase in degradation of AHR triggered by exposure to TCDD, AHR protein levels recovered close to control levels in SD rats and to or beyond (depending on assay) control levels in H/W rats. In L-E rats, the AHR protein did not recover even after 10 days.

The TCDD doses that we employed (5 or 50 $\mu\text{g/kg}$) were not notably different from the dose range (0.2 to 25 $\mu\text{g/kg}$) used in studies that reported down-regulation. By immuno-

blotting, we predominantly measured AHR in cytosol and nuclear extracts rather than whole tissue lysates. As shown (Fig. 4), receptor levels in cytosols were highly correlated with those in whole tissue lysates from the same animal ($r^2 = 0.945$, $N = 8$), indicating that quantitation of AHR in either preparation is reliable.

The high correlation ($r^2 = 0.739$, $N = 90$) between measurements by ligand binding and immunoblotting in our study confirms that increases in AHR levels are genuine. Although the magnitude of change measured by the two techniques was different (particularly with the high-dose treatment), the pattern of change and resulting conclusions were the same. Theoretically, at the high dose, the administered TCDD may occupy a greater fraction of cytosolic AHR sites, rendering these unavailable for detection by the radioligand binding assay without affecting measurements made by immunoblotting. In spite of this potential underestimate of AHR levels by the radioligand binding assay, increases in receptor levels over the time course were still observed.

One of our incidental findings was that only a small fraction of the total cellular AHR pool appeared to be localized in the nucleus post-TCDD, especially with high-dose TCDD. Nevertheless, nuclear AHR levels clearly were sufficient to drive and maintain *CYP1A1* gene expression. Rucci and Gasiewicz [41] have shown that, in hamsters, approximately 30% of the total receptor pool is associated with the nuclear fraction within hours of treatment with [^3H]TCDD (10 $\mu\text{g/kg}$, i.p.); this gradually declined to about 5% over several weeks with maintenance of maximal *CYP1A1* induction. It remains unclear whether nuclear AHR levels are low in TCDD-treated rats because (i) only a small fraction is translocated, and (ii) TCDD promotes degradation of the receptor. Based on the precedent from cell culture, nuclear receptor would be expected to be vulnerable to proteolysis. The fate of the nuclear receptor has been investigated in cell culture [42] but remains uninvestigated *in vivo*.

Although AHR levels can be altered significantly by TCDD exposure *in vivo*, TCDD has little influence on the receptor's dimerization partner, ARNT, either at the level of immunoreactive protein [current study; 24,36,40] or mRNA [current study].

The up-regulation that we observed *in vivo* stands in sharp contrast to what we, and others [25–28,43–45], observed in cell culture in which treatment with AHR agonists causes rapid and prolonged depletion of AHR protein. This depletion has recently been shown to be due to proteolytic degradation [26] via the ubiquitin–proteasome complex triggered by exposure of the AHR to ligands such as TCDD [43,45,46]. Degradation by the ubiquitin–proteasome complex probably occurs in tissues *in vivo* as well as in various cell types in culture; no *in vivo* experiments have demonstrated this yet. It should not be ignored that cell culture models, although valuable tools, sometimes reflect a distorted or incomplete picture of normal physiologic re-

sponses. Even if TCDD does enhance AHR degradation in liver *in vivo*, TCDD also seems to increase receptor synthesis to an extent that not only replenishes depleted AHR over the course of a few days, but also causes a net increase in the total content of AHR at a dose that does not produce appreciable initial depletion.

Our study significantly extends previous *in vivo* studies of the effect of TCDD on AHR levels since, in addition to quantitating the level of receptor protein by both immunoblotting and ligand binding, we concurrently measured the level of AHR mRNA in the same tissue. Other studies reported the effect of TCDD on either AHR mRNA levels and/or AHR protein levels but not both in the same tissue [36,47–49]. Our previous experiments in cell culture show that the level of AHR mRNA is not altered by TCDD in mouse Hepa-1 hepatoma cells [26], nor in human LS180 colon carcinoma cells [37]. Our current *in vivo* study shows clearly that, in all cases of increased AHR protein, be it in the form of recovery (50 $\mu\text{g/kg}$ dose) or net increase over basal levels (5 $\mu\text{g/kg}$ dose), there is an accompanying increase in AHR mRNA in all strains tested. This suggests a pre-translational mechanism for restoration or elevation of AHR levels. Since TCDD likely triggers both degradation of its receptor and elevation of steady-state receptor mRNA, it is not surprising that AHR mRNA and protein levels are not quantitatively correlated.

CYP1A1 mRNA was highly induced by the first day of TCDD treatment. In contrast, the elevation in AHR mRNA was not significant in any rat strain at either dose until at least 4 days after TCDD exposure. CYP1A1 induction has been documented extensively to be a direct primary response mediated by binding of ligand \cdot AHR \cdot ARNT complexes to DREs in the 5'-flanking region of responsive genes [1–3]. The delayed onset of elevated AHR mRNA suggests a mechanism different from that of CYP1A1 induction. Alternatively, the apparent lag in AHR mRNA accumulation may reflect a different stability of the AHR mRNA compared with CYP1A1 mRNA. The rat AHR 5'-flanking region remains to be sequenced, but DREs are known to exist in the 5'-flanking sequences of the *Ahr* gene from mice [50] and humans.¹ It is not yet known if those DREs can contribute to enhancing AHR expression in cells exposed to agonists such as TCDD.

Does up-regulation of the AHR have any impact on responsiveness of the animal to TCDD? There are no *in vivo* data to answer this question. Receptor theory predicts that an increase in cellular receptor abundance can enhance responsiveness to ligand by increasing the maximal response and/or shifting the dose–response curve to the left depending on the nature of the stimulus–response cascade [51]. Andersen and Barton [52] provide a quantitative model in which “autoinduction” of the AHR by TCDD can promote steeper dose–response curves to TCDD by switch-

ing the cell to a “highly ligand-responsive” state as a form of positive feedback. In cultured cells, the exposure to ligand provokes a dramatic depletion of AHR via proteolysis; this may desensitize the cell to excessive stimulation by AHR agonists. Our experiments *in vivo* demonstrate that, even though a ligand may trigger initial depletion, a single dose of TCDD has the ability to restore or elevate AHR levels over several days. Since binding of TCDD to the AHR is the first essential step to mediating toxicity, a relatively modest change in total AHR content in a cell or tissue could confer a substantial increase in sensitivity of some responses to AHR ligands.

In cell culture it has been demonstrated that “superinduction” of CYP1A1 by TCDD can be produced by blocking degradation of the AHR protein [53]. In the current *in vivo* study, CYP1A1 induction was comparable among strains regardless of the fluctuations in AHR protein, suggesting that this response is largely unaffected by changes in AHR levels. CYP1A1 induction is one of many biochemical responses to TCDD and, although well characterized, is probably not involved directly in acute TCDD toxicity [54]. The molecular events leading to TCDD toxicity remain unclear. The number of receptors required for a particular response are likely to be endpoint dependent; therefore, the impact of fluctuations in AHR levels on toxic responses will depend largely on the nature of the molecular cascade(s) leading to toxicity. The extent to which elevated receptor levels increase sensitivity to TCDD *in vivo* will be challenging to assess in whole-animal experiments but is worthy of investigation.

In our study, the AHR was up-regulated by TCDD in all three rat strains. The lack of a clear relationship between patterns of AHR regulation and toxic endpoints (in terms of body weight, liver weight, or LD_{50}) indicates that inherent strain susceptibility likely is not attributable to differential regulation of the AHR by TCDD. The extraordinary resistance of the Han/Wistar (*Kuopio*) strain to lethal effects of TCDD cannot be attributed to a failure to up-regulate the receptor. Nevertheless, the sensitive Long-Evans (*Turku AB*) and Sprague Dawley rat strains have higher total hepatic levels of AHR than the resistant H/W strain, both before and after TCDD exposure. The relatively low abundance of AHR in H/W rats may contribute to their resistance to the lethal effects of TCDD.

Our multiple-dose, multiple-endpoint, multiple-strain study demonstrates unequivocally that, in addition to initial depletion, the AHR is also up-regulated by TCDD. Consequently, the widely held view that TCDD produces only down-regulation of the AHR *in vivo* is inadequate, as are the speculated physiological implications when they are confined exclusively to down-regulation.

Acknowledgments

We thank Ms. Arja Tamminen and Ms. Minna Voutilainen for excellent technical assistance. This work was supported by

¹ Harper PA, personal communication. Cited with permission.

the Medical Research Council of Canada/Canadian Institutes of Health Research (A.B.O.); the Natural Sciences and Engineering Research Council of Canada (M.A.F.); the Academy of Finland, Research Council for Health (Grant No. 43984) and the Finnish Research Program for Environmental Health [SYTTY] (Grant No. 42386) (J.T. and R.P.).

References

- [1] Denison MS, Phelen D, Elferink CJ. The Ah receptor signal transduction pathway. In: Denison MS, Helferich WG, editors. *Xenobiotics, receptors and gene expression*. Philadelphia: Taylor & Francis, 1998. p. 3–33.
- [2] Whitlock JP. Induction of cytochrome P4501A1. *Annu Rev Pharmacol Toxicol* 1999;39:103–25.
- [3] Nebert DW, Roe AL, Dieter MZ, Solis WA, Yang Y, Dalton TP. Role of the aromatic hydrocarbon receptor and [Ah] gene battery in the oxidative stress response, cell cycle control, and apoptosis. *Biochem Pharmacol* 2000;59:65–85.
- [4] Pohjanvirta R, Tuomisto J. Short-term toxicity of 2,3,7,8-tetrachlorodibenzo-*p*-dioxin in laboratory animals: effects, mechanisms, and animal models. *Pharmacol Rev* 1994;46:483–549.
- [5] Okey AB, Riddick DS, Harper PA. The Ah receptor: mediator of the toxicity of 2,3,7,8-tetrachlorodibenzo-*p*-dioxin (TCDD) and related compounds. *Toxicol Lett* 1994;70:1–22.
- [6] Poland A, Glover E. 2,3,7,8-Tetrachlorodibenzo-*p*-dioxin: segregation of toxicity with the Ah locus. *Mol Pharmacol* 1980;17:86–94.
- [7] Tuomisto JT, Viluksela M, Pohjanvirta R, Tuomisto J. The AH receptor, and a novel gene determine acute toxic responses to TCDD: segregation of the resistant alleles to different rat lines. *Toxicol Appl Pharmacol* 1999;155:71–81.
- [8] Fernandez-Salguero PM, Hilbert DM, Rudikoff S, Ward JM, Gonzalez FJ. Aryl-hydrocarbon receptor-deficient mice are resistant to 2,3,7,8-tetrachlorodibenzo-*p*-dioxin-induced toxicity. *Toxicol Appl Pharmacol* 1996;140:173–9.
- [9] Lahvis GP, Bradfield CA. *Ahr* null alleles: distinctive or different? *Biochem Pharmacol* 1998;56:781–7.
- [10] Hahn ME. The aryl hydrocarbon receptor: a comparative perspective. *Comp Biochem Physiol C Pharmacol Toxicol Endocrinol* 1998;121:23–53.
- [11] Okey AB, Vella LM, Harper PA. Detection and characterization of a low affinity form of cytosolic Ah receptor in livers of mice nonresponsive to induction of cytochrome P₁-450 by 3-methylcholanthrene. *Mol Pharmacol* 1989;35:823–30.
- [12] Poland A, Palen D, Glover E. Analysis of the four alleles of the murine aryl hydrocarbon receptor. *Mol Pharmacol* 1994;46:915–21.
- [13] Pohjanvirta R, Unkila M, Tuomisto J. Comparative acute lethality of 2,3,7,8-tetrachlorodibenzo-*p*-dioxin (TCDD), 1,2,3,7,8-pentachlorodibenzo-*p*-dioxin and 1,2,3,4,7,8-hexachlorodibenzo-*p*-dioxin in the most TCDD-susceptible and the most TCDD-resistant rat strain. *Pharmacol Toxicol* 1993;73:52–6.
- [14] Pohjanvirta R, Viluksela M, Tuomisto JT, Unkila M, Karasinska J, Franc M-A, Holowenko M, Giannone JV, Harper PA, Tuomisto J, Okey AB. Physicochemical differences in the AH receptors of the most TCDD-susceptible and the most TCDD-resistant rat strains. *Toxicol Appl Pharmacol* 1999;155:82–95.
- [15] Pohjanvirta R, Wong JMY, Li W, Harper PA, Tuomisto J, Okey AB. Point mutation in intron sequence causes altered carboxyl-terminal structure in the aryl hydrocarbon receptor of the most 2,3,7,8-tetrachlorodibenzo-*p*-dioxin-resistant rat strain. *Mol Pharmacol* 1998;54:86–93.
- [16] Okey AB, Vella LM. Elevated binding of 2,3,7,8-tetrachlorodibenzo-*p*-dioxin and 3-methylcholanthrene to the Ah receptor in hepatic cytosols from phenobarbital-treated rats and mice. *Biochem Pharmacol* 1984;33:531–8.
- [17] Denomme MA, Leece B, Li A, Towner R, Safe S. Elevation of 2,3,7,8-tetrachlorodibenzo-*p*-dioxin (TCDD) polychlorinated biphenyls. Structure-activity relationships. *Biochem Pharmacol* 1986;35:277–82.
- [18] Göttlicher M, Cikryt P. Induction of the aromatic hydrocarbon receptor by *trans*-4-acetylaminostilbene in rat liver. Comparison with other aromatic amines. *Carcinogenesis* 1987;8:1021–3.
- [19] Landers JP, Birse LM, Nakai JS, Winhall MJ, Bunce NJ. Chemically induced hepatic cytosol from the Sprague-Dawley rat: evidence for specific binding of 2,3,7,8-tetrachlorodibenzo-*p*-dioxin to components kinetically distinct from the Ah receptor. *Toxicol Lett* 1990;51:295–302.
- [20] Landers JP, Winhall MJ, McCready TL, Sanders DA, Rasper D, Nakai JS, Bunce NJ. Characterization of an inducible aryl hydrocarbon receptor-like protein in rat liver. *J Biol Chem* 1991;266:9471–80.
- [21] Benedetti L, MacCormack LS, Bunce NJ. Characterization of a phenobarbital-inducible Ah receptor-like protein in the Sprague-Dawley rat. *Arch Biochem Biophys* 1994;309:1–9.
- [22] Sloop TC, Lucier GW. Dose-dependent elevation of Ah receptor binding by TCDD in rat liver. *Toxicol Appl Pharmacol* 1987;88:329–37.
- [23] Bunce NJ, Landers JP, Schneider UA, Safe SH, Zacharewski TR. Chlorinated *trans* stilbenes: competitive binding to the AH receptor, induction of cytochrome P-450 monooxygenase activity, and partial 2,3,7,8-TCDD antagonism. *Toxicol Environ Chem* 1990;28:217–29.
- [24] Pollenz RS, Santostefano MJ, Klett E, Richardson VM, Necela B, Birnbaum LS. Female Sprague-Dawley rats exposed to a single oral dose of 2,3,7,8-tetrachlorodibenzo-*p*-dioxin exhibit sustained depletion of aryl hydrocarbon receptor protein in liver, spleen, thymus, and lung. *Toxicol Sci* 1998;42:117–28.
- [25] Giannone JV, Okey AB, Harper PA. Characterization of polyclonal antibodies to the aromatic hydrocarbon receptor. *Can J Physiol Pharmacol* 1995;73:7–17.
- [26] Giannone JV, Li W, Probst M, Okey AB. Prolonged depletion of AH receptor without alteration of receptor mRNA levels after treatment of cells in culture with 2,3,7,8-tetrachlorodibenzo-*p*-dioxin. *Biochem Pharmacol* 1998;55:489–97.
- [27] Pollenz RS. The aryl-hydrocarbon receptor, but not the aryl-hydrocarbon receptor nuclear translocator protein, is rapidly depleted in hepatic and nonhepatic culture cells exposed to 2,3,7,8-tetrachlorodibenzo-*p*-dioxin. *Mol Pharmacol* 1996;49:391–8.
- [28] Prokipcak RD, Okey AB. Downregulation of the Ah receptor in mouse hepatoma cells treated in culture with 2,3,7,8-tetrachlorodibenzo-*p*-dioxin. *Can J Physiol Pharmacol* 1991;69:1204–10.
- [29] Singh SS, Perdew GH. Alterations in the Ah receptor level after staurosporine treatment. *Arch Biochem Biophys* 1993;305:170–5.
- [30] Döhr O, Sinning R, Vogel C, Münzel P, Abel J. Effect of transforming growth factor- β_1 on expression of aryl hydrocarbon receptor and genes of Ah gene battery: clues for independent down-regulation in A549 cells. *Mol Pharmacol* 1997;51:703–10.
- [31] Vartiainen T, Lampi P, Tuomisto JT, Tuomisto J. Polychlorodibenzo-*p*-dioxin, and polychlorodibenzofuran concentrations in human fat samples in a village after pollution of drinking water with chlorophenols. *Chemosphere* 1995;30:1429–38.
- [32] Pollenz RS, Sattler CA, Poland A. The aryl hydrocarbon receptor and aryl hydrocarbon receptor nuclear translocator protein show distinct subcellular localizations in Hepa 1c1c7 cells by immunofluorescence microscopy. *Mol Pharmacol* 1994;45:428–38.
- [33] Mason ME, Okey AB. Cytosolic and nuclear binding of 2,3,7,8-tetrachlorodibenzo-*p*-dioxin to the Ah receptor in extra-hepatic tissues of rats and mice. *Eur J Biochem* 1982;123:209–15.
- [34] Bradford MM. A rapid, and sensitive method for the quantitation of microgram quantities of protein utilizing the principle of protein-dye binding. *Anal Biochem* 1976;72:248–54.

- [35] Holmes JL, Pollenz RS. Determination of aryl hydrocarbon receptor nuclear translocator protein concentration and subcellular localization in hepatic and nonhepatic cell culture lines: development of quantitative Western blotting protocols for calculation of aryl hydrocarbon receptor and aryl hydrocarbon receptor nuclear translocator protein in total cell lysates. *Mol Pharmacol* 1997;52:202–11.
- [36] Sommer RJ, Sojka KM, Pollenz RS, Cooke PS, Peterson RE. Ah receptor and ARNT protein and mRNA concentrations in rat prostate: effects of stage of development and 2,3,7,8-tetrachlorodibenzo-*p*-dioxin treatment. *Toxicol Appl Pharmacol* 1999;155:177–89.
- [37] Li W, Harper PA, Tang BK, Okey AB. Regulation of cytochrome P450 enzymes by aryl hydrocarbon receptor in human cells: CYP1A2 expression in the LS180 colon carcinoma cell line after treatment with 2,3,7,8-tetrachlorodibenzo-*p*-dioxin or 3-methylcholanthrene. *Biochem Pharmacol* 1998;56:599–612.
- [38] de Morais SM, Giannone JV, Okey AB. Photoaffinity labeling of the Ah receptor with 3-[³H]methylcholanthrene and formation of a 165-kDa complex between the ligand-binding subunit and a novel cytosolic protein. *J Biol Chem* 1994;269:12129–36.
- [39] Murphy LD, Herzog CE, Rudick JB, Fojo AT, Bates SE. Use of the polymerase chain reaction in the quantitation of *mdr-1* gene expression. *Biochemistry* 1990;29:10351–6.
- [40] Roman BL, Pollenz RS, Peterson RE. Responsiveness of the adult male rat reproductive tract to 2,3,7,8-tetrachlorodibenzo-*p*-dioxin exposure: Ah receptor and ARNT expression, CYP1A1 induction, and Ah receptor down-regulation. *Toxicol Appl Pharmacol* 1998;150:228–39.
- [41] Rucci G, Gasiewicz TA. *In vivo* kinetics, and DNA-binding properties of the Ah receptor in the golden Syrian hamster. *Arch Biochem Biophys* 1988;265:197–207.
- [42] Pollenz RS, Barbour ER. Analysis of the complex relationship between nuclear export and aryl hydrocarbon receptor-mediated gene regulation. *Mol Cell Biol* 2000;20:6095–104.
- [43] Ma Q, Baldwin KT. 2,3,7,8-Tetrachlorodibenzo-*p*-dioxin-induced degradation of aryl hydrocarbon receptor (AhR) by the ubiquitin-proteasome pathway. Role of the transcription activation and DNA binding of AhR. *J Biol Chem* 2000;275:8432–8.
- [44] Reick M, Robertson RW, Pasco DS, Fagan JB. Down-regulation of nuclear aryl hydrocarbon receptor DNA-binding and transactivation functions: requirement for a labile or inducible factor. *Mol Cell Biol* 1994;14:5653–60.
- [45] Roberts BJ, Whitelaw ML. Degradation of the basic helix-loop-helix/Per-ARNT-Sim homology domain dioxin receptor via the ubiquitin/proteasome pathway. *J Biol Chem* 1999;274:36351–6.
- [46] Davarinos NA, Pollenz RS. Aryl hydrocarbon receptor imported into the nucleus following ligand binding is rapidly degraded via the cytoplasmic proteasome following nuclear export. *J Biol Chem* 1999;274:28708–15.
- [47] Abnet CC, Tanguay RL, Hahn ME, Heideman W, Peterson RE. Two forms of aryl hydrocarbon receptor type 2 in rainbow trout (*Oncorhynchus mykiss*). Evidence for differential expression and enhancer specificity. *J Biol Chem* 1999;274:15159–66.
- [48] Huang P, Rannug A, Ahlbom E, Håkansson H, Ceccatelli S. Effect of 2,3,7,8-tetrachlorodibenzo-*p*-dioxin on the expression of cytochrome P450 1A1, the aryl hydrocarbon receptor, and the aryl hydrocarbon receptor nuclear translocator in rat brain and pituitary. *Toxicol Appl Pharmacol* 2000;169:159–67.
- [49] Tanguay RL, Abnet CC, Heideman W, Peterson RE. Cloning and characterization of the zebrafish (*Danio rerio*) aryl hydrocarbon receptor. *Biochim Biophys Acta* 1999;1444:35–48.
- [50] Schmidt JV, Carver LA, Bradfield CA. Molecular characterization of the murine *Ahr* gene. Organization, promoter analysis, and chromosomal assignment. *J Biol Chem* 1993;268:22203–9.
- [51] Kenakin TP. Pharmacologic analysis of drug-receptor interaction. Philadelphia: Lippincott-Raven Publishers, 1997.
- [52] Andersen ME, Barton HA. Biological regulation of receptor-hormone complex concentrations in relation to dose-response assessments for endocrine-active compounds. *Toxicol Sci* 1999;48:38–50.
- [53] Ma Q, Renzelli AJ, Baldwin KT, Antonini JM. Superinduction of *CYP1A1* gene expression. Regulation of 2,3,7,8-tetrachlorodibenzo-*p*-dioxin-induced degradation of Ah receptor by cycloheximide. *J Biol Chem* 2000;275:12676–83.
- [54] Poland A, Knutson JC. 2,3,7,8-Tetrachlorodibenzo-*p*-dioxin, and related halogenated aromatic hydrocarbons: examination of the mechanism of toxicity. *Annu Rev Pharmacol Toxicol* 1982;22:517–54.